Probing the Oligomeric Assemblies of Pea Porphobilinogen Synthase by Analytical Ultracentrifugation[†]

Bashkim Kokona,[‡] Daniel J. Rigotti,[‡] Andrew S. Wasson,[‡] Sarah H. Lawrence,[§] Eileen K. Jaffe,[§] and Robert Fairman*,[‡]

Department of Biology, Haverford College, 370 Lancaster Avenue, Haverford, Pennsylvania 19041, and Fox Chase Cancer Center, 333 Cottman Avenue, Philadelphia, Pennsylvania 19111

ABSTRACT: The enzyme porphobilinogen synthase (PBGS) can exist in different nonadditive homooligomeric assemblies, and under appropriate conditions, the distribution of these assemblies can respond to ligands such as metals or substrate. PBGS from most organisms was believed to be octameric until work on a rare allele of human PBGS revealed an alternate hexameric assembly, which is also available to the wild-type enzyme at elevated pH [Breinig, S., et al. (2003) *Nat. Struct. Biol. 10*, 757−763]. Herein, we establish that the distribution of pea PBGS quaternary structures also contains octamers and hexamers, using both sedimentation velocity and sedimentation equilibrium experiments. We report results in which the octamer dominates under purification conditions and discuss conditions that influence the octamer: hexamer ratio. As predicted by PBGS crystal structures from related organisms, in the absence of magnesium, the octameric assembly is significantly destabilized, and the oligomeric distribution is dominated largely by the hexameric assembly. Although the PBGS hexamer-to-octamer oligomeric rearrangement is well documented under some conditions, both assemblies are very stable (under AU conditions) in the time frame of our ultracentrifuge experiments.

The enzyme porphobilinogen synthase (PBGS),[1] also known as 5-aminolevulinic acid dehydratase (ALAD), catalyzes the first common step in the biosynthesis of tetrapyrroles including heme, chlorophyll, vitamin B_{12}, and cofactor F_{430} (*1*). The pea (*Pisum sativum*) PBGS enzyme has been a useful model system to explore metal ion regulation of enzyme activity (*2*). It has been proposed that part of the regulatory mechanism for pea PBGS activity involves dynamic control of its oligomeric assembly (*3*), and Mg^{2+} has been implicated in the quaternary structure of PBGS from species such as *Escherichia coli*, *Pseudomonas aeruginosa*, and *Chlorobium vibrioforme* (*4−6*).

The dynamic nature of the quaternary structure of pea PBGS under assay conditions results in a protein concentration-dependent specific enzyme activity (*2*). This unusual kinetic phenomenon was originally interpreted as due to an *additive* equilibrium of oligomeric assemblies that could include less active dimers and tetramers along with active octamers (*2*); the octamer was well established from the first crystal structure of PBGS (*7*). A more recent structural hypothesis ascribes the low activity of pea PBGS to a hexameric state, which is *nonadditive* relative to the octamer, and analogous to the recently determined crystal structure of a hexameric form of human PBGS (*3*). The interconversion of the human PBGS octamer and hexamer is now well established to proceed via a mechanism of dissociation to a dimeric assembly, conformational change at the level of the dimer, and reassociation to the alternate higher order oligomer (*8, 9*). The interpretation of pea PBGS as assembling to either an octamer or a hexamer, as illustrated in Figure 1, is supported by structural arguments based on (1) the location of an allosteric magnesium binding site in other PBGS (*5*), (2) native gel electrophoresis showing that removal of magnesium stabilizes the putative hexamer relative to the putative octamer (*3*), and (3) mutagenesis studies on human PBGS designed to mimic removal of the allosteric magnesium (*10*). However, prior to the current work, there was no independent sizing or crystallographic data demonstrating the existence of both octameric and hexameric assemblies for pea PBGS. The current work uses analytical ultracentrifugation techniques to provide a rigorous biophysical test of this model. Analytical ultracentrifugation is used to evaluate the effects of Mg^{2+} on the quaternary structure of pea PBGS, a question that has previously been addressed using native gel electrophoresis (*3, 4*).

* To whom correspondence should be addressed. E-mail: rfairman@haverford.edu. Telephone: (610) 896-4205. Fax: (610) 896-4963.

[‡] Haverford College.

[§] Fox Chase Cancer Center.

[1] Abbreviations: ALA, 5-aminolevulinic acid; AU, analytical ultracentrifugation; βME, β-mercaptoethanol; BTP, 1,3-bis[tris(hydroxymethyl)methylaminopropane]; DTT, dithiothreitol; EDTA, ethylenediaminetetraacetic acid; PAGE, polyacrylamide gel electrophoresis, PBGS, porphobilinogen synthase; SDS, sodium dodecyl sulfate; SE, sedimentation equilibrium; SV, sedimentation velocity; Tris, tris(hydroxymethyl)aminomethane.
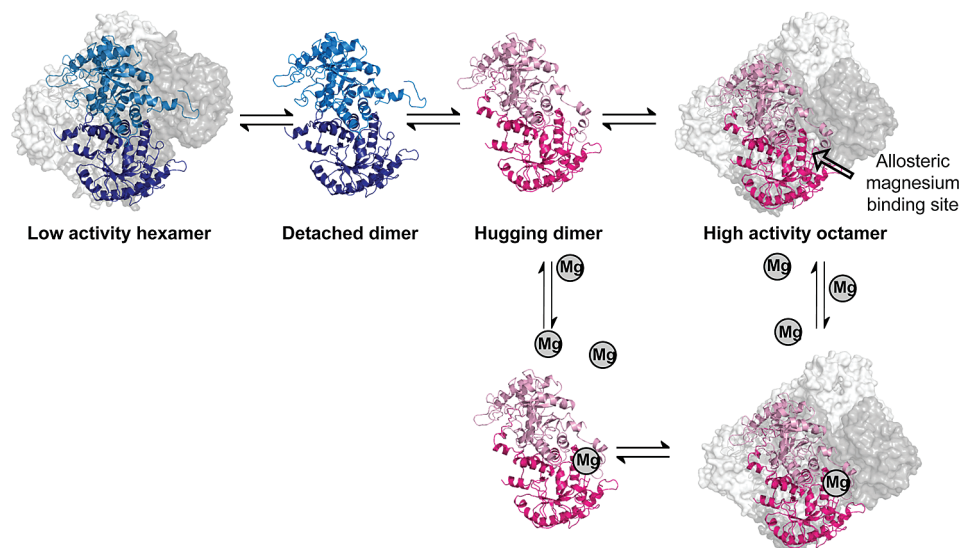
FIGURE 1: The different oligomeric assemblies of PBGS. The PBGS equilibrium ensemble of quaternary structure forms is illustrated using homology models of pea PBGS. For most species, the asymmetric unit of the crystal structure is an asymmetric homodimer (*3, 5, 6, 27*). The hexamer and its asymmetric unit, the detached dimer (based on PDB code 1PV8), are shown in two shades of blue. The octamer and its asymmetric unit, the hugging dimer (based on PDB code 1GZG), are shown in two shades of pink. For the octamer, the dimers assemble at a 90° rotation around a central axis; for the hexamer, the dimers assemble at a 120° rotation around a central axis. The octamer contains a phylogenetically variable binding site for an allosteric magnesium ion. This ion binds to the arm-to-barrel interface that is unique to the octamer; the allosteric magnesium binding site is not present in the hexamer (*3, 22*).

MATERIALS AND METHODS

Enzyme Preparation. The pea PBGS used in our experiments was prepared from an artificial gene encoding a 330 residue enzyme without the putative chloroplast transit peptide; the protein was expressed in *E. coli* and readily purified in 100 mg quantities (*2*). We chose to work with a mutant form of the pea protein in which a surface cysteine has been replaced with an alanine (C326A). The wild-type protein is prone to intersubunit disulfide cross-linking through Cys326. The C326A mutation has been shown to have no effect on enzymatic activity, and it is unlikely to affect the structure of the protein (*2*). C326A pea PBGS was purified as described (*2*) with an additional Sephacryl S-300 gel filtration step using a buffer comprised of 0.1 M Tris-HCl, pH 8.5, 10 mM MgCl$_2$, and 10 mM βME. The concentrated pool from that column yielded our stock concentrations of 21.3 mg/mL, which were flash frozen and stored at −80 °C.

Polyacrylamide Gel Electrophoresis (PAGE). All electrophoresis was performed using the PhastGel system (GE BioScience) at 15 °C, and all molecular mass markers, buffers, and gels were purchased from GE Bioscience and used according to the manufacturer's guidelines. For the SDS gel, purified pea PBGS (12 mg/mL) was mixed in a 1:1 ratio with Laemmli buffer containing 5% β-mercaptoethanol and boiled for 15 min. The sample was further diluted in Laemmli buffer to 3 mg/mL such that the loading volume of 4 μL contained 12 μg of protein. The molecular mass standards contained phosphorylase B (97 kDa), albumin (66 kDa), ovalbumin (45 kDa), carbonic anhydrase (30 kDA), trypsin inhibitor (20.1 kDa), and α-lactalbumin (14.4 kDa). The sample and standards were resolved on a 12.5% polyacrylamide gel with SDS buffer strips.

For the native PAGE experiments, samples were diluted to the working concentration using 0.1 M Tris-HCl, pH 8.5, and 10 mM MgCl$_2$. To determine the effects of the addition of MgCl$_2$ or ALA, the hexameric starting sample was prepared by dialyzing 50 μL of pea PBGS (10 mg/mL) in minidialysis units (Pierce) against 200 mL of 10 mM BTP-HCl, pH 8.5. Dialysis was allowed to proceed for 14 h at 4 °C with stirring, and the sample was then stored at 4 °C until analysis. Any further dilutions of the protein were performed using the dialysis buffer as the diluent. Reagents added to the protein samples were also prepared in the dialysis buffer. Incubations of protein with these reagents were performed at 1 mg/mL PBGS for 5 min at 37 °C. The samples were resolved on a 12.5% polyacrylamide gel with native buffer strips. The 4 μL loading volume of each lane contained approximately 4 μg of PBGS.

Ultracentrifugation Sample Preparation. Stocks were thawed at room temperature and then dialyzed overnight at 4 °C using Slide-A-Lyzer dialysis cassettes (Pierce) in the presence of 0.1 M BTP-HCl, pH 8.5, 0.1 mM DTT, and 10 mM MgCl$_2$. Removal of MgCl$_2$ or readdition of MgCl$_2$ was accomplished by dialysis in the absence or presence of this reagent. Dialysis buffers were prepared with MilliQ purified water followed by filtration using 0.2 μm filters. Protein concentration was determined by measuring tryptophan and tyrosine absorption using an extinction coefficient of $(Y)_{280nm}$ = 1235 cm^{-1} M^{-1} and $(W)_{280nm}$ = 5690 cm^{-1} M^{-1} (*11*).

Analytical Ultracentrifugation. All experiments were performed using a Beckman model Optima XL-A analytical ultracentrifuge equipped with an An-60 Ti rotor. SV experiments used two-channel Epon, charcoal-filled centerpieces with 1.2 cm path lengths containing 450 μL samples and 500 μL buffer references. Sedimentation velocity was typically assayed at a speed of 30000 or 50000 rpm at 20 °C. Absorbance data were collected using a radial step size of 0.003 cm. Samples were monitored at a wavelength of 278 nm with a starting absorbance value of around 1.0. The rotor temperature was equilibrated to the running temperature prior to spinning of the rotor. Scans were initiated at the beginning of the run and were collected with no time delay between

scans. Values for the C326A pea PBGS molecular mass (polypeptide MW = 36693 Da), partial specific volume, solvent densities, and viscosities were calculated using Sednterp (v.1.08) (*12*). SV data were analyzed using the DCDT+ program, using the $g(s^*)$ method (v.2.0.4; John Philo, Thousand Oaks, CA) (*13*). The number of sedimentation profiles used for analysis was defined by the constraints specified by the algorithm used to fit the data to avoid boundary spreading due to diffusion. Molecular masses and the standard errors for analyzed species were calculated from $s_{20,w}$, and $D_{20,w}$ coefficients using the DCDT+ program. Additional analysis of SV data (including $c(s)$ analysis and analysis using noninteracting discrete models) and generation of synthetic data were done using Sedfit (*14, 15*). SE experiments used six-channel Epon charcoal-filled centerpieces, with 1.2 cm path lengths and column heights between 0.25 and 0.3 cm, containing 110 μL samples and 125 μL buffer references. Absorbance scans were measured at speeds of 8000, 10000, and 12000 rpm at 20 °C, using a radial step size of 0.001 cm and an absorbance wavelength of 278 nm. Equilibrium data were truncated using the WinReedit (v.0.999) program (1998) and analyzed using either Win-NonLin (v.1.035; 1997) (*16*) or an SE curve-fitting procedure encoded into Igor v.4.05A Carbon (1988, 2002; WaveMetrics, Inc.), obtained from Jim Lear (*17*). The Igor procedure has implemented mixture models by using multiexponential expressions in which the amplitudes of each individual exponential can be treated as independent variable parameters. In addition, the procedure allows for the assessment of mass balance and can test the degree of mass conservation in global fitting routines. We found that integrating the concentration profiles from the beginning of each data set to an assumed bottom of the column revealed good agreement in mass balance and allowed us to calculate the weight percent of each species in two-component mixtures. The baseline absorbances were insignificant relative to the absorbances of the samples, and thus no special procedure was used in fitting baseline absorbances. These were treated as independent parameters for each data set used in the global fitting routine and showed no systematic variation.

RESULTS

Analysis of Pea PBGS in the Presence of 10 mM MgCl$_2$. Our overall goals in this study were twofold: (1) to rigorously establish the identity and heterogeneity of oligomeric assemblies in pea PBGS and (2) to characterize the role of Mg^{2+} in the oligomeric distribution and stability. Due to the irreversible nature of the PBGS catalyzed reaction and the aromatic (UV absorbing) nature of the product porphobilinogen, all AU analyses were carried out in the absence of substrate.

Given the dynamic nature of the distribution of human PBGS quaternary structure assemblies that has been observed recently (*8–10*) and the protein concentration-dependent specific activity observed for PBGS from other species (*2, 18, 19*), we were intrigued by the native PAGE experiments that suggest that pea PBGS can form hexamers and octamers (*3*). As illustrated in Figure 2A, pea PBGS that is homogeneous by SDS gel electrophoresis resolves into two bands by native PAGE. Based on the mobility of the native PAGE bands relative to the known octamer and hexamer of human PBGS
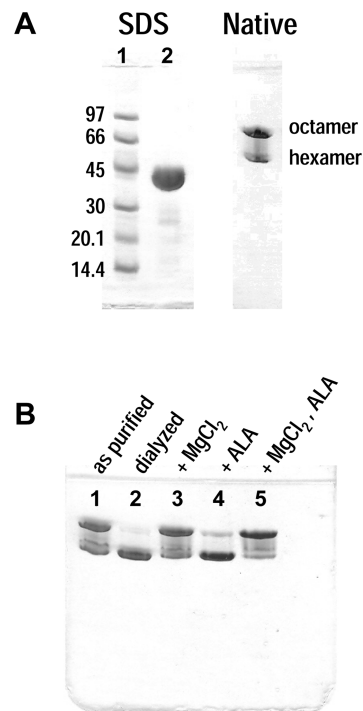

FIGURE 2: Electrophoretic analysis of pea PBGS. (A) PAGE analysis of purified pea PBGS. SDS lane 1, molecular mass markers (masses shown in kDa); SDS lane 2, pea PBGS (3 mg/mL) as purified (100 mM Tris-HCl, pH 8.5, 10 mM MgCl$_2$); Native, pea PBGS (1 mg/mL) as purified. (B) Native PAGE analysis of pea PBGS (1 mg/mL). Lane 1, pea PBGS as purified; lane 2, pea PBGS dialyzed vs 10 mM BTP, pH 8.5; lane 3, the sample shown in lane 2 with 10 mM MgCl$_2$ added in the protein dilution step; lane 4, the sample shown in lane 2 with 1 mM ALA added in the protein dilution step; lane 5, the sample shown in lane 2 with 10 mM MgCl$_2$ and 1 mM ALA added in the protein dilution step.

protein, we proposed that pea PBGS can form hexamers and octamers (*3*). We first tested for this polydispersity using sedimentation velocity (SV) experiments.

Samples of the enzyme were diluted to three different working concentrations (30, 10, and 3 μM subunit) from stock concentrations of 21 mg/mL (57 μM) protein and dialyzed overnight at 4 °C against 0.1 M BTP-HCl, pH 8.5, 0.1 mM DTT, and 10 mM MgCl$_2$ and then subjected to ultracentrifugation at 30000 or 50000 rpm at 20 °C over sufficient time to generate a well-defined set of sedimentation boundary profiles. Under these conditions, there was no dependence of sedimentation as a function of protein concentration. A single-species model, using the program dCdT+, revealed a reasonable fit to the data with some nonrandom distribution of the residuals in comparing the model with the data (Figure 3). Assuming a single species for all three concentrations tested, we obtained an $s_{20,w}$ of 10.94 ± 0.04 S. When coupled with the best-fit value for the diffusion parameter ($(3.61 \pm 0.01) \times 10^{-7}$ cm^2 s^{-1}), we obtain an average molecular mass of 276500 ± 9000 Da. Thus, the experimentally determined molecular mass is consistent with the protein being largely an octamer (expected octamer molecular mass is 293544 Da) with minimal contribution from other species. The nonrandom residuals do however suggest minor heterogeneity in the samples, and we noted an improvement in the fit when using a three-species model (Figure 3). The additional species detected include a smaller species and a larger species (possibly
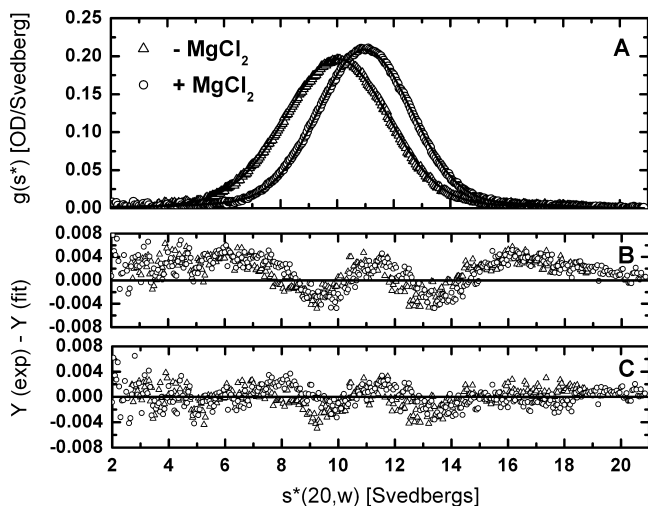
FIGURE 3: Sedimentation velocity analysis of PBGS in the presence and absence of Mg^{2+}. The $g(s^*)$ distribution of $s^*_{20,w}$ including a fit using either a single-species model or a three-species model is shown. Solution conditions: 34 μM C326A pea PBGS in 0.1 M BTP, pH 8.5, 0.1 mM DTT, and $\pm$10 mM $MgCl_2$, at 20 °C; data collected at 30000 rpm. (A) The data are shown fit with the three-species model. (B) The residuals from fitting using single-species models display a nonrandom distribution, suggesting an inferior fit to this model. (C) A marked improvement is observed in the residuals from fitting using three-species models.

aggregated protein), but these species represent only 1−2% of the total absorbance. We note that the lack of concentration dependence to the sedimentation rate is consistent with an ideal single species but could also reflect a nonequilibrating mixture of hexamers and octamers. Further analysis led to the surprising conclusion that we could not distinguish mixtures of hexamers and octamers (whose presence is suggested from the SE data described below) from a single dominant species; we tackle this problem in the Discussion section.

Switching to SE experiments, we first tested the time required to reach an equilibrium distribution of oligomeric species by sedimenting the protein at several concentrations at 8000 rpm, 20 °C, and collecting data every 4 h for comparison purposes. Using the WinMatch program, we found no difference in sedimentation between 16 and 20 h; thus all data were collected using a minimum of 16 h of equilibration time. We collected data at three protein concentrations and at three rotor speeds. The apparent molecular mass from simultaneous fitting of the three speeds for each protein concentration, as a single ideal species, reveals an average falling somewhere between the expected hexamer and octamer molecular masses (Table 1). There is minimal speed dependence to the molecular masses, suggesting that there is a single major species in solution, presumably the octamer, as suggested from the sedimentation velocity experiment. Furthermore, we see little, if any, protein concentration dependence to the apparent molecular mass (Table 1), suggesting that, if multiple species are present, they are not in dynamic equilibrium under the conditions of SE data collection. Prior work under enzyme turnover conditions showed a protein concentration-dependent specific activity only at protein concentrations below 1 μM ($\sim$36 μg/mL) (2). Those data were obtained in the presence of substrate and at 37 °C, which are factors that are expected to influence assembly/disassembly kinetics; we have previ-

Table 1: SE Analysis of Molecular Mass as a Function of Pea PBGS Protein Concentration, Assuming a Single Ideal Species

	speed (rpm)			
sample[a]	8000	10000	12000	global[b]
30 μM	266500[c]	257000	253000	257000 ± 7500
10 μM	274000	272000	273000	273200 ± 8000
3 μM	269000	273000	266000	269000 ± 10000
all concns[d]	270000	263000	259500	264000 ± 5500

[a] 0.1 M BTP-HCl, pH 8.5, 0.1 mM DTT, and 10 mM $MgCl_2$ collected at 20 °C. [b] The term "global" refers to global fits across all speeds for a given concentration. The last row of this column represents a global fit to all three speeds and three concentrations simultaneously. [c] All molecular masses are reported in daltons. The theoretical monomer molecular mass of pea PBGS is 36693 Da. [d] The row labeled "all concns" contains global fits across all concentrations for a given speed.

Table 2: Model Analysis of Pea PBGS from SE Experiments with and without $MgCl_2$, Using an Unweighted Reduced χ^2 as a Measure of Goodness of Fit[a]

model	$+MgCl_2$ ($\times 10^{-3}$)	$-MgCl_2$ ($\times 10^{-3}$)
hexamer	14	3.89
octamer	4.65	10.5
2,8	1.80/2.19[b]	2.04/6.30[b]
4,8	1.65/1.90	2.03/3.07
6,8	1.58[c]	2.16[d]

[a] 0.1 M BTP-HCl, pH 8.5, and 0.1 mM DTT ± 10 mM $MgCl_2$, 20 °C. Model analysis is based on global fitting to the three protein concentrations and three speeds, as reported in Table 1. [b] When two values are presented, the first value assumes a nonequilibrating mixture model and the second value assumes an equilibrium model. In each model, the species are held fixed as appropriate multiples of the monomeric molecular mass. [c] Fitting of the data with inclusion of mass balance constraints reveals 65% octamer and 35% hexamer by weight. [d] Fitting of the data with inclusion of mass balance constraints reveals 25% octamer and 75% hexamer by weight.

ously established that there are conditions where the human PBGS hexamer is stable, or perhaps metastable, until substrate, which stabilizes the octamer assembly, is added and a hexamer to octamer reequilibration is initiated (8−10).

Model analysis of the SE data for pea PBGS in the presence of 10 mM Mg^{2+} was carried out using all speeds and protein concentrations simultaneously in a global curve-fitting procedure, and the results are presented in Table 2. Hexamer and octamer single-species models fit the data reasonably well with a significant improvement for the octamer model, based on evaluation of unweighted reduced χ^2 values, a measure of goodness of fit. Two-species models (in which each species is represented as a fixed multiple of the monomeric molecular mass) resulted in further improvement in the fits, even when compared to a model-free single ideal species analysis (in which the molecular mass is treated as a floating parameter). In considering different two-species models, we tested the goodness of fit of both equilibrium and mixture models. In every case, the mixture models gave better fits to the data than the corresponding equilibrium models, consistent with the lack of concentration dependence that we reported in Table 1. The best fit to the data was for a model that included only hexamers and octamers (Table 2, column 1, Figure 4, and Figure S1 in Supporting Information), with the octamer as the major species.

Analysis of Pea PBGS Following Removal and Readdition of the Mg^{2+}. Mg^{2+} was removed by dialysis into the parent buffer without $MgCl_2$ in order to observe its effects on the distribution between the hexamer and octamer assemblies using SV experiments. In this case, we observed a sedimen-
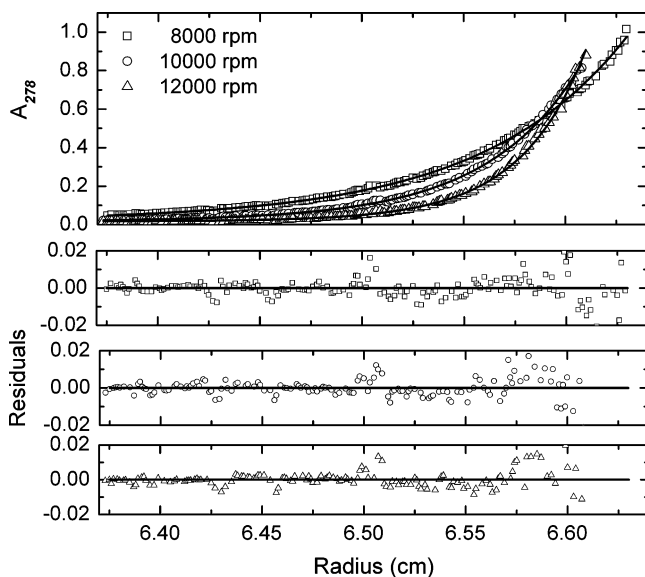
FIGURE 4: Sedimentation equilibrium analysis of PBGS in the presence of MgCl$_2$. SE data are shown fit with a hexamer−octamer model where the hexamer and octamer are treated as nonequilibrating mixtures. The fit shown is that from simultaneous analysis of three protein concentrations (3, 10, and 30 μM subunits) each collected at three rotor speeds. Data were collected at 8000, 10000, and 12000 rpm. The fits to all of the data are provided in Figure S1 in the Supporting Information. Sample conditions: 10 μM C326A pea PBGS in 0.1 M BTP-HCl, pH 8.5, 0.1 mM DTT, and 10 mM MgCl$_2$, at 20 °C.

tation boundary with an $s_{20,w}$ value of 10.03 ± 0.04 S from a $g(s^*)$ analysis, which is independent of protein concentration (using 3, 10, and 30 μM) and is significantly smaller than that observed prior to dialysis in the presence of MgCl$_2$ (Figure 3). This s-value, when combined with the best-fit diffusion coefficient ($D_{20,w} = (4.34 ± 0.17) \times 10^{-7}$ cm^2 s^{-1}), provided a molecular mass of 212000 ± 9000 Da, or close to that expected for a hexamer. However, as we observed for the sedimentation behavior in the presence of Mg^{2+}, the residuals from the single-species fit show a nonrandom component (Figure 3). The residuals are essentially random in a three-species analysis. While the fitting parameters are highly correlated, resulting in ill-determined s-values, we can conclude that the second species has a higher s-value than that expected for a hexamer, suggestive of small amounts of octamer present. This is confirmed in the SE analysis presented below.

SE analysis of pea PBGS after dialysis to remove MgCl$_2$ confirms the drop in size observed in the SV experiment. The apparent molecular mass from a global single-species analysis of data collected at multiple protein concentrations and rotor speeds is 236500 ± 7500 Da (Table 3), a value in close agreement with that expected for the theoretical hexamer molecular mass of 220158 Da. As we saw with the protein in the presence of Mg^{2+}, the apparent molecular mass is independent of either protein concentration or rotor speed. This observation supports the conclusion that the sample is dominated by one species and that any additional species are not in dynamic equilibrium with the dominant species during the time frame of the analysis. Model analysis suggests that a two-species hexamer/octamer model provides a significantly improved fit to the data over hexamer, octamer, or model-free single-species models (Table 2, Figure 5, and Figure S2 in Supporting Information). While

Table 3: Molecular Mass Analysis of Pea PBGS from SE Experiments Testing the Effect of Magnesium Depletion on Pea PBGS Quaternary Structure Assemblies, Assuming a Single Ideal Species

	speed (rpm)			
sample[a]	8000	10000	12000	global[b]
30 μM PBGS	233000[c]	227000	229000	230000 ± 9000
10 μM PBGS	260000	254000	249000	252000 ± 10000
3 μM PBGS	232000	226000	219000	223000 ± 17000
all concns[d]	237500	237000	236000	236500 ± 7500

[a] Samples of pea PBGS were dialyzed against 0.1 M BTP-HCl, pH 8.5, and 0.1 mM DTT at 4 °C prior to SE analysis and run at 20 °C. [b] The term "global" refers to global fits across all speeds for a given concentration. The last row of this column represents an global fit to all three speeds and three concentrations simultaneously. [c] All molecular masses are reported in daltons. [d] The row labeled "all concns" contains global fits across all concentrations for a given speed.
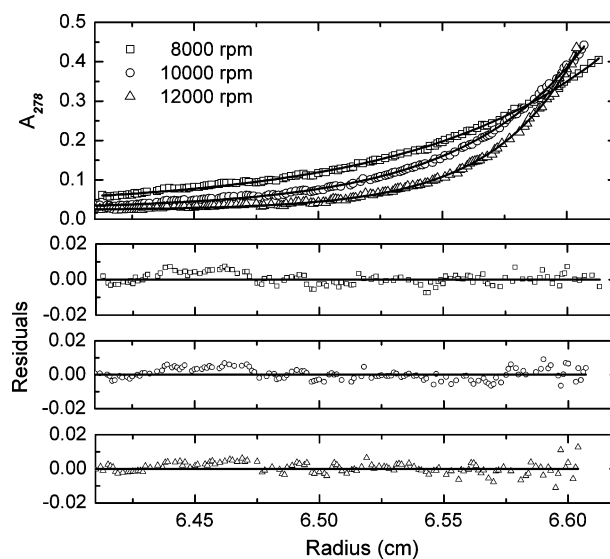

FIGURE 5: Sedimentation equilibrium analysis of PBGS in the absence of MgCl$_2$. The data are shown fit with a hexamer−octamer model where the hexamer and octamer are irreversible mixtures. The fit shown is that from simultaneous analysis of three protein concentrations (3, 10, and 30 μM) each collected at three rotor speeds. Data were collected at 8000, 10000, and 12000 rpm. The fits to all of the data are provided in Figure S2 in the Supporting Information. Sample conditions: 10 μM C326A pea PBGS in 0.1 M BTP-HCl, pH 8.5, and 0.1 mM DTT, at 20 °C.

dimer/octamer or tetramer/octamer models (in which the two oligomers are treated as nonequilibrating mixtures) fit equally well, we can rule these models out because they both predict that the octamer would be the major species. For example, the ratio of tetramer to octamer (0.3:0.7) is inconsistent with the ratios of the smaller and larger species from either the SV analysis or the native PAGE experiments presented here and in our earlier work (3). Furthermore, the calculated frictional coefficient (f/f_0 ratio) for a hexamer, using the experimentally determined s-value, is 1.34, which is consistent with that expected for a hydrated hexamer; in contrast, this ratio is only 1.04 for a tetramer state, thus providing further support for hexamer assemblies dominating the sample in the absence of Mg^{2+}.

We also tested if reintroducing 10 mM MgCl$_2$ could result in regeneration of octamer assemblies. Samples were initially dialyzed overnight at 4 °C in the absence of MgCl$_2$, tested for their sedimentation behavior as described above, and then redialyzed back into 10 mM MgCl$_2$ for further analysis. A

complete recovery of the original apparent molecular mass is observed (265500 ± 4500 Da based on global data fitting) and shows the same lack of protein concentration or rotor speed dependence as observed in the samples freshly dialyzed into $MgCl_2$ (Table S1 in Supporting Information). Thus, we conclude that magnesium is critical for controlling the ratio of hexamers and octamers.

Native PAGE Analysis. Under assay conditions, substrate turnover can play a role in shifting the oligomeric distribution to favor the octamer for human and *E. coli* PBGS (*4, 8*). This is presumably related to the fact that PBGS crystal structures with a closed active site lid have additional octamer specific subunit interactions relative to the open-lid conformation (*9*). Our prior studies on the effects of Mg^{2+} and ALA on the oligomeric distribution of PBGS from several species had been carried out by native PAGE (*3, 4*). In order to confirm and expand these earlier findings for pea PBGS, we repeated the analysis using native PhastGels (Figure 2B). The predominance of octamer in the purified proteins, which is in the presence of magnesium, in the PhastGel system (Figure 2B, lane 1) is similar to that seen in our AU experiments described above and in previously published native gels (*3*). Removal of Mg^{2+} by dialysis at low ionic strength (Figure 2B, lane 2) shows a dramatic redistribution to the hexamer, also consistent with our AU experiments. Subsequent addition of $MgCl_2$ to the dialyzed protein shifts the equilibrium to favor formation of octamers (Figure 2B, lane 3). The addition of ALA to the dialyzed protein in the absence of $MgCl_2$ causes only minimal conversion of hexamers to octamers (Figure 2B, lane 4); however, concurrent addition of ALA and $MgCl_2$ to the dialyzed protein induces almost total conversion to octamers. Under conditions where the sample contains a large fraction of octamer (Figure 2B, lanes 1, 3, and 5), the hexamer band runs as a doublet. We find that a small percentage of octameric pea PBGS converts to hexamer during electrophoresis; this is most clearly observed during two-dimensional native PAGE as recently published (*20*). This hexamer that is formed during the experiment migrates at a retarded position relative to the PBGS that went into the gel as a hexamer, resulting in the appearance of a doublet.

DISCUSSION

Through a combination of sedimentation velocity and sedimentation equilibrium analytical ultracentrifugation studies, we have established that the pea PBGS protein is largely octameric in the presence of 10 mM $MgCl_2$ (*2*). In the absence of added $MgCl_2$, the enzyme forms hexamers. We find that this process is reversible since adding back $MgCl_2$ restores the octamer assembly.

This system has required careful AU analysis since nonadditive oligomeric states, being similar in their molecular masses (220 kDa for the hexamer vs 293 kDa for the octamer), pose challenges in deconvoluting their contributions to heterogeneity. While SV methods are particularly sensitive to sample heterogeneity, we have found that distinguishing hexamers from octamers in our system is much more challenging and is further exacerbated by the fact that these behave as independent species and thus cannot be probed simply using protein concentration profiling. We did note heterogeneity in the SV samples, using either dCdT+

(Figure 3) or SedFit (analysis not shown), but the species resulting in this heterogeneity were either much smaller than a hexamer/octamer or much larger than an octamer and represent minute (1−2%) amounts. These additional species are likely to reflect either very small amounts of contaminating protein or minor aggregation. Having accounted for these, the fits to the SV data resulted in random residuals. There was no improvement in our ability to resolve hexamers from octamers at the highest speeds recommended with the standard four-hole rotor fitted with Epon centerpieces.

In order to explore this problem more deeply, we created synthetic data to represent a 50:50 mixture of the two species using 10.03 and 10.94 S as measures of the *s*-values for the hexamer and octamer, respectively. We also incorporated the typical signal to noise present using an absorbance detection system. In general, we found that the ability of either the dCdT+ or SedFit algorithms to unambiguously assign the fraction of hexamer and octamer present in such a predefined mixture was quite poor since random residuals were obtained from a wide range of hexamer and octamer distributions. A quantitative comparison of the rmsd values for various models, using either the noninteracting discrete species algorithm in Sedfit or the $g(s^*)$ multiple species algorithm in dCdT+ is shown in Table S2 (Supporting Information). In the case of the Sedfit analysis of the synthetic data, we found that we could recover a proportion of 46:54 for the hexamer:octamer species with best-fit *s*-values of 10.08 and 10.98 S (while keeping the molecular masses fixed at the theoretical hexamer and octamer values), which compared well to the input values. However, the rmsd of this fit was almost identical to that using other ratios of hexamer and octamer and, more importantly, to an unconstrained single-species model. In applying this approach to the pea PBGS data, we found that the rmsd value for a fit to a single-species model was identical to that found for different proportions of hexamer and octamer. Similar observations were made using dCdT+. Thus, we conclude that there is significant ambiguity in establishing such heterogeneity in our SV experiments.

The question of hexamer/octamer heterogeneity was better resolved using SE experiments. We were able to see evidence for both hexamers and octamers in the presence and absence of Mg^{2+}, but in each case, one of the components dominated the mixture. Thus, quantifying the contribution of the minor species was difficult. Most problematic was establishing the oligomeric state of the smaller species under octamer-favoring conditions, principally because there was insufficient absorbance to unambiguously establish the assembly state from a limited panel of experimental conditions. This analysis was rendered more difficult because there was no apparent exchange between the hexamer and octamer states, as evidenced by a lack of concentration dependence between the two species. However, careful global analysis of data collected at multiple concentrations and multiple rotor speeds allowed us to establish the presence of these two species unambiguously. The SV and SE experiments, taken in total, have allowed us to elucidate the role of Mg^{2+} in regulating the distribution of an unusual nonadditive mixture of protein assemblies, involving hexamers and octamers.

The role of Mg^{2+} in the assembly of hexamers and octamers in the pea PGBS is not unprecedented. Metal ions play diverse roles in the majority of PBGS that have been

studied. In many cases, Zn^{2+} binding at the active site is critical for activity (*7, 21−24*). In other cases Mg^{2+} and some monovalent salts have been shown to be required for activity and are presumed to bind at or near the active site (*2, 19, 25, 26*). In addition, many PBGS are regulated through the binding of metal at an allosteric site; these are best characterized as Mg^{2+} sites (*22, 27*). Plant PBGS enzymes appear to require only Mg^{2+} for enzymatic activity (*2, 26*), and three types of magnesium sites are suggested from the kinetic behavior of pea PBGS (*2*). A catalytically essential magnesium ($K_d \sim$ 35 μM) is putatively at the active site. An allosteric magnesium ($K_d \sim$ 2 mM), the location of which is illustrated in Figure 1, was first observed in the crystal structures of *P. aeruginosa* PBGS (*5*). This site is at a subunit interface that is present in the octameric assembly but not in the hexameric assembly. It is the existence of this allosteric Mg^{2+} site that would lead one to ask whether Mg^{2+} is a structural requirement for formation of the pea PBGS octamer. Prior work showed that removal of Mg^{2+} with EDTA favors smaller assemblies for the PBGS of both pea and *E. coli* (*3, 4*). The third magnesium of pea PBGS is inhibitory ($K_d > $ 10 mM); its location and mechanism are not characterized. The optimal enzyme activity for the chloroplast-located pea PBGS requires Mg^{2+} concentrations in the physiologically relevant range of 1−10 mM (*2*). The current work explores the relationship between Mg^{2+} and the specific oligomeric assemblies of pea PBGS. We chose to perform the current studies at 10 mM Mg^{2+} to address the hexamer octamer equilibrium and avoid substantial population of the inhibitory Mg^{2+} binding site. Here we find that, in the absence of substrate, magnesium stabilizes the octameric assembly as predicted from the known location of the allosteric magnesium at a subunit interface that is unique to the octamer.

The existence of nonadditive quaternary structure assemblies for PBGS and the realization that a rearrangement between octamer and hexamer constitutes the structural basis for allosteric regulation of plant PBGS by Mg^{2+} led us to compare the regulation of PBGS with the classic models of allostery (Monod−Wyman−Changeux vs Koshland−Nemethy−Filmer *28, 29*). These classic models do not consider a situation wherein oligomer dissociation is a *required* component of the allosteric mechanism, as it is for PBGS. Hence, we introduced the term morpheein, presented it as a structural basis for allosteric regulation, and suggested that quaternary structure rearrangements similar to that experienced by PBGS may be more common than currently believed (*30*). We propose that analytical ultracentrifugation data, fitted to nonadditive mixtures or equilibrium models, will assist in the characterization of proteins that can exist as an ensemble of morpheein forms.

ACKNOWLEDGMENT

SUPPORTING INFORMATION AVAILABLE

All of the data sets used for the global fitting of the sedimentation equilibrium data in the presence (Figure S1) and absence (Figure S2) of Mg^{2+} and tables presenting the analysis of SE data upon readdition of Mg^{2+} (Table S1) and the analysis of synthetic SV data (Table S2). This material is available free of charge via the Internet at http://pubs.acs.org.

REFERENCES

1. Battersby, A. R. (2000) Tetrapyrroles: the pigments of life. *Nat. Prod. Rep. 17*, 507–526.
2. Kervinen, J., Dunbrack, R. L., Jr., Litwin, S., Martins, J., Scarrow, R. C., Volin, M., Yeung, A. T., Yoon, E., and Jaffe, E. K. (2000) Porphobilinogen synthase from pea: expression from an artificial gene, kinetic characterization, and novel implications for subunit interactions. *Biochemistry 39*, 9018–9029.
3. Breinig, S., Kervinen, J., Stith, L., Wasson, A. S., Fairman, R., Wlodawer, A., Zdanov, A., and Jaffe, E. K. (2003) Control of tetrapyrrole biosynthesis by alternate quaternary forms of porphobilinogen synthase. *Nat. Struct. Biol. 10*, 757–763.
4. Jaffe, E. K., Ali, S., Mitchell, L. W., Taylor, K. M., Volin, M., and Markham, G. D. (1995) Characterization of the role of the stimulatory magnesium of Escherichia coli porphobilinogen synthase. *Biochemistry 34*, 244–251.
5. Frankenberg, N., Erskine, P. T., Cooper, J. B., Shoolingin-Jordan, P. M., Jahn, D., and Heinz, D. W. (1999) High resolution crystal structure of a Mg^{2+}-dependent porphobilinogen synthase. *J. Mol. Biol. 289*, 591–602.
6. Coates, L., Beaven, G., Erskine, P. T., Beale, S. I., Avissar, Y. J., Gill, R., Mohammed, F., Wood, S. P., Shoolingin-Jordan, P., and Cooper, J. B. (2004) The X-ray structure of the plant like 5-aminolaevulinic acid dehydratase from Chlorobium vibrioforme complexed with the inhibitor laevulinic acid at 2.6 Å resolution. *J. Mol. Biol. 342*, 563–570.
7. Erskine, P. T., Senior, N., Awan, S., Lambert, R., Lewis, G., Tickle, I. J., Sarwar, M., Spencer, P., Thomas, P., Warren, M. J., Shoolingin-Jordan, P. M., Wood, S. P., and Cooper, J. B. (1997) X-ray structure of 5-aminolaevulinate dehydratase, a hybrid aldolase. *Nat. Struct. Biol. 4*, 1025–1031.
8. Tang, L., Stith, L., and Jaffe, E. K. (2005) Substrate induced interconversion of protein quaternary structure isoforms. *J. Biol. Chem. 280*, 15786–15793.
9. Selwood, T., Tang, L., Lawrence, S. H., Anokhina, Y., and Jaffe, E. K. (2008) Kinetics and thermodynamics of the interchange of the morpheein forms of human porphobilinogen synthase. *Biochemistry 47*, 3245–3257.
10. Tang, L., Breinig, S., Stith, L., Mischel, A., Tannir, J., Kokona, B., Fairman, R., and Jaffe, E. K. (2006) Single amino acid mutations alter the distribution of human porphobilinogen synthase quaternary structure isoforms (morpheeins). *J. Biol. Chem. 281*, 6682–6690.
11. Edelhoch, H. (1967) Spectroscopic determination of tryptophan and tyrosine in proteins. *Biochemistry 6*, 1948–1954.
12. Laue, T. M., Shah, B. D., Ridgeway, T. M., and Pelletier, S. L. (1992) Computer-Aided Interpretation of Analytical Sedimentation Data for Proteins, in *Analytical Ultracentrifugation in Biochemistry and Polymer Science* (Harding, S. E., Rowe, A. J., and Horton, J. C., Eds.) The Royal Society of Chemistry, Cambridge.
13. Philo, J. S. (2000) A method for directly fitting the time derivative of sedimentation velocity data and an alternative algorithm for calculating sedimentation coefficient distribution functions. *Anal. Biochem. 279*, 151–163.
14. Brown, P. H., and Schuck, P. (2008) A new adaptive grid-size algorithm for the simulation of sedimentation velocity profiles in analytical ultracentrifugation. *Comput. Phys. Commun. 178*, 105–120.
15. Schuck, P. (2000) Size-distribution analysis of macromolecules by sedimentation velocity ultracentrifugation and lamm equation modeling. *Biophys. J. 78*, 1606–1619.
16. Johnson, M. L., Correia, J. J., Yphantis, D. A., and Halvorson, H. R. (1981) Analysis of data from the analytical ultracentrifuge by nonlinear least-squares techniques. *Biophys. J. 36*, 575–588.

17. Arkin, M., and Lear, J. D. (2001) A new data analysis method to determine binding constants of small molecules to proteins using equilibrium analytical ultracentrifugation with absorption optics. *Anal. Biochem. 299*, 98–107.

18. Bollivar, D. W., Clauson, C., Lighthall, R., Forbes, S., Kokona, B., Fairman, R., Kundrat, L., and Jaffe, E. K. (2004) Rhodobacter capsulatus porphobilinogen synthase, a high activity metal ion independent hexamer. *BMC Biochem. 5*, 17.

19. Petrovich, R. M., Litwin, S., and Jaffe, E. K. (1996) Bradyrhizobium japonicum porphobilinogen synthase uses two Mg(II) and monovalent cations. *J. Biol. Chem. 271*, 8692–8699.

20. Lawrence, S. H., Ramirez, U. D., Tang, L., Fazliyez, F., Kundrat, L., Markham, G. D., and Jaffe, E. K. (2008) Shape shifting leads to small-molecule allosteric drug discovery. *Chem. Biol. 15*, 586–596.

21. Cheh, A., and Neilands, J. B. (1973) Zinc, an essential metal ion for beef liver delta-aminolevulinate dehydratase. *Biochem. Biophys. Res. Commun. 55*, 1060–1063.

22. Jaffe, E. K. (2003) An unusual phylogenetic variation in the metal ion binding sites of porphobilinogen synthase. *Chem. Biol. 10*, 25–34.

23. Jaffe, E. K., and Hanes, D. (1986) Dissection of the early steps in the porphobilinogen synthase catalyzed reaction. Requirements for Schiff's base formation. *J. Biol. Chem. 261*, 9348–9353.

24. Wetmur, J. G., Bishop, D. F., Cantelmo, C., and Desnick, R. J. (1986) Human delta-aminolevulinate dehydratase: nucleotide sequence of a full-length cDNA clone. *Proc. Natl. Acad. Sci. U.S.A. 83*, 7703–7707.

25. Boese, Q. F., Spano, A. J., Li, J. M., and Timko, M. P. (1991) Aminolevulinic acid dehydratase in pea (Pisum sativum L.). Identification of an unusual metal-binding domain in the plant enzyme. *J. Biol. Chem. 266*, 17060–17066.

26. Senior, N. M., Brocklehurst, K., Cooper, J. B., Wood, S. P., Erskine, P., Shoolingin-Jordan, P. M., Thomas, P. G., and Warren, M. J. (1996) Comparative studies on the 5-aminolaevulinic acid dehydratases from Pisum sativum, Escherichia coli and Saccharomyces cerevisiae. *Biochem. J. 320* (Part 2), 401–412.

27. Kervinen, J., Jaffe, E. K., Stauffer, F., Neier, R., Wlodawer, A., and Zdanov, A. (2001) Mechanistic basis for suicide inactivation of porphobilinogen synthase by 4,7-dioxosebacic acid, an inhibitor that shows dramatic species selectivity. *Biochemistry 40*, 8227–8236.

28. Koshland, D. E., Jr., Nemethy, G., and Filmer, D. (1966) Comparison of experimental binding data and theoretical models in proteins containing subunits. *Biochemistry 5*, 365–385.

29. Monod, J., Wyman, J., and Changeux, J. P. (1965) On the nature of allosteric transitions: a plausible model. *J. Mol. Biol. 12*, 88–118.

30. Jaffe, E. K. (2005) Morpheeins—a new structural paradigm for allosteric regulation. *Trends Biochem. Sci. 30*, 490–497.

Table S1. Molecular mass analysis of pea PBGS from SE experiments testing the re-addition of magnesium on pea PBGS quaternary structure assemblies, assuming a single ideal species. [2]

Sample/Speed	8,000 rpm	10,000 rpm	12,000 rpm	Global[2]
30 μM PBGS	269,000[3]	264,000	257,000	265,000±5,000
10 μM PBGS	275,000	267,500	266,000	268,000±7,000
3 μM PBGS	260,000	253,500	239,000	248,000±10,000
3 conc'ns[4]	269,000	266,000	260,000	265,500±4,500

[1]Samples were dialyzed identically as described in Note 2 in Table 3 and then $MgCl_2$ was dialyzed back in for four hours just prior to the ultracentrifuge run.

[2]The term, "global" refers to global fits across all speeds for a given concentration. The last row of this column represents an global fit to all three speeds and three concentrations simultaneously.

[3]All molecular masses are reported Daltons.

[4]The row labeled "all conc'ns" contains global fits across all concentrations for a given speed.

Table S2. Root mean square deviation (RMSD) analysis of non-interacting discrete models as fit using SV synthetic data created by Sedfit.[1]

Model	Sedfit algorithm		dCdT+ algorithm	
	RMSD $(x10^{-3})$	Best fit s-values (S)	RMSD $(x10^{-3})$	Best fit s-values (S)
Single species[2]	3.6	10.49	2.0	10.97
Hexamer[3]	4.2		2.8	
Octamer[3]	8.4		6.3	
Hexamer:octamer[4]	2.8 (46:54)	10.08/10.98	1.8 (49:51)	10.49/11.42
50:50 hexamer:octamer[5]	2.8	10.04/10.95	1.8	10.50/11.42
20:80 hexamer:octamer	3.0	10.31/11.26	2.2	9.89/11.20
80:20 hexamer:octamer	3.7	9.48/10.72	2.0	10.78/11.74

[1]Synthetic data were created as described in Materials and Methods.

[2]The single species model was carried out with no constraints on molecular mass.

[3]The hexamer and octamer models constrain the molecular mass to their theoretical values.

[4]The proportion of hexamer and octamer is treated as a fitting parameter. The molecular masses for hexamer and octamer are fixed. The proportions are shown in parentheses next to the RMSD values.

[5]The fits represent molecular masses fixed at the theoretical values for hexamer and octamer and with s-values treated as fitting parameters.
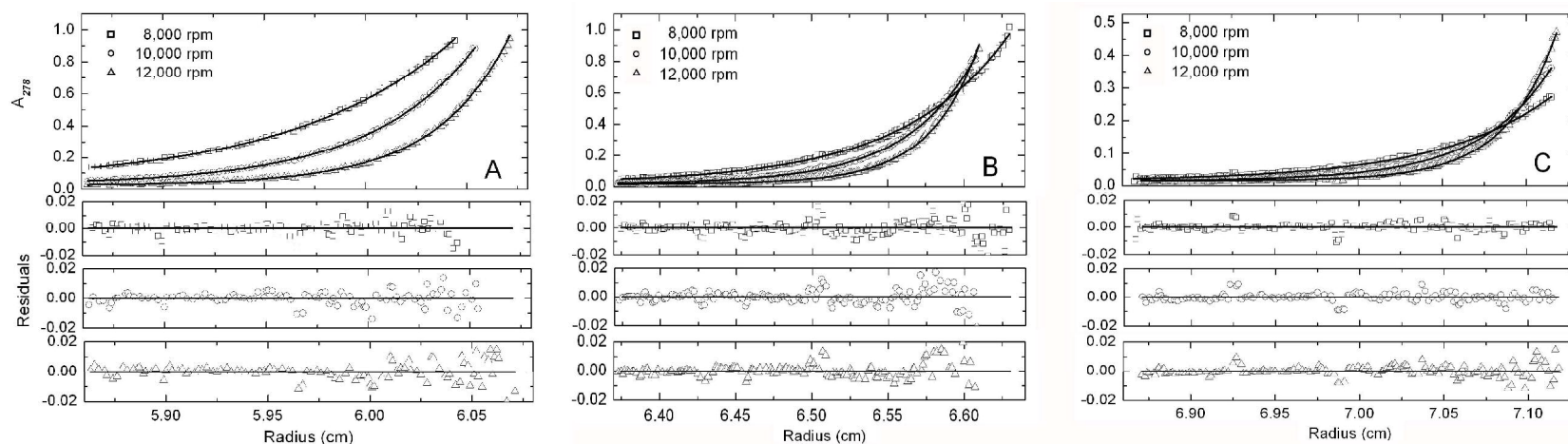
Figure S1.

Figure S1. Sedimentation equilibrium analysis of PBGS in the presence of $MgCl_2$. SE data are shown fit with a hexamer-octamer model where the hexamer and octamer are independent states. The fits shown are that from simultaneous analysis of three protein concentrations: (A) 3 μM subunits; (B) 10 μM subunits; and (C) 30 μM subunits, each collected at three rotor speeds. Sample conditions: 0.1 M BTP-HCl, pH 8.5, 0.1 mM DTT, and 10 mM $MgCl_2$, at 20°C.
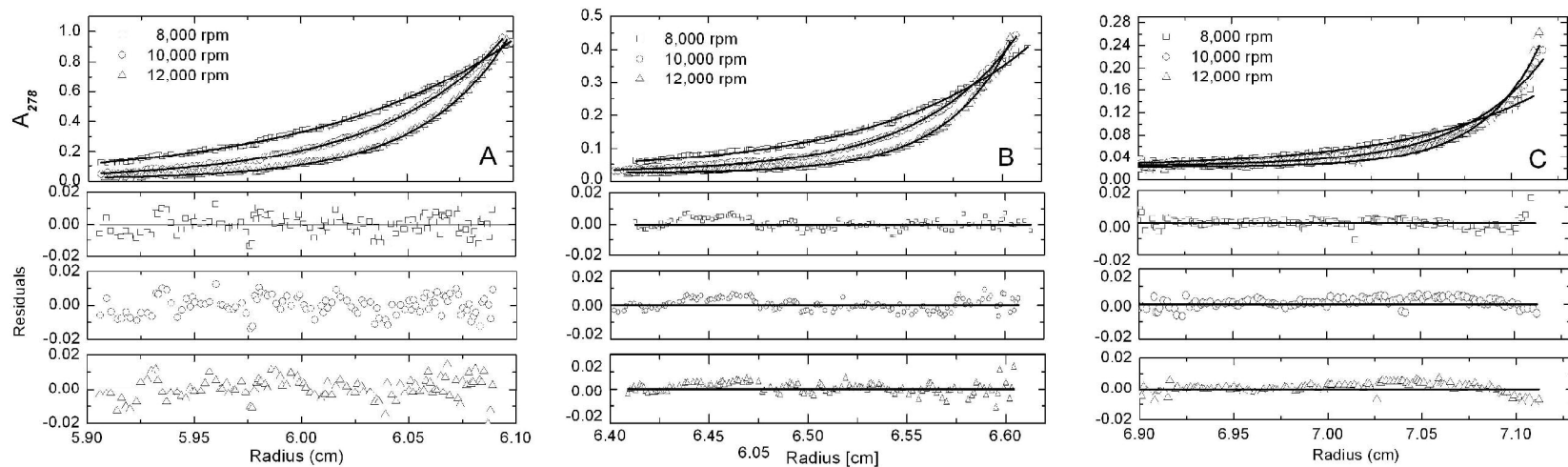
Figure S2.

Figure S2. Sedimentation equilibrium analysis of PBGS in the absence of MgCl$_2$. SE data are shown fit with a hexamer-octamer

model where the hexamer and octamer are independent states. The fits shown are that from simultaneous analysis of three protein

concentrations: (A) 3 μM subunits; (B) 10 μM subunits; and (C) 30 μM subunits, each collected at three rotor speeds. Sample

conditions: 0.1 M BTP-HCl, pH 8.5, and 0.1 mM DTTat 20°C.